JOURNAL OF
EMERGING INVESTIGATORS

Article

Effect of fuel density and temperature on helium-3 fusion reaction rates in stellar cores

Maximus Widmaier[1], Christine Celestino[1]
[1] Juan Diego Catholic High School, Draper, Utah

SUMMARY

Fusion energy—the same energy that powers the Sun—is a promising avenue for sustainable, green energy. However, current fusion reactors face two major challenges: high energy usage and fast material degradation. Present designs consume over 60 times more energy than they produce and become inoperable after only 5–10 years of full-time use. Unlike reactors, stars operate efficiently at much lower temperatures, even for reactions that are far more difficult to achieve. This stellar efficiency arises from the interplay of high temperatures and fuel density, and understanding how stellar fusion operates can inform new approaches to reactor design. Currently, no simple and direct model exists to describe how temperature and fuel density jointly determine fusion reaction rates. Based on the standard fusion reaction rate equation, we hypothesized that density would have a quadratic, temperature-independent effect on reaction rates. To test this hypothesis, we analyzed stellar cores using simulations to isolate and quantify the effects of temperature and density on fusion activity. The results contradicted the initial hypothesis. At low temperatures, increasing density either reduced or had no effect on reaction rates. However, as temperatures increased, density had an increasingly positive effect on reaction rates. This indicates that, contrary to the hypothesis, temperature and density interact to maximize fusion efficiency rather than contributing independently. Fusion energy will usher in a new age of sustainable, green energy. Since mainstream fusion reactors primarily focus on maximizing either temperature or density, we must focus on optimizing both to produce more efficient reactors sooner.

INTRODUCTION

Fusion is the process of combining lighter elements, such as hydrogen, into heavier elements like helium (1). This differs from fission, in which heavy atoms—such as uranium—are split into lighter atoms (2). Fusion reactions are extremely energy-dense, as a small portion of the reactants' mass is converted directly into energy, in accordance with Einstein's mass-energy equation, $E = mc^2$ (3).

Current fusion research focuses primarily on deuterium and tritium—two isotopes of hydrogen with one and two neutrons, respectively (3). Conversely, stellar fusion involves a series of three different fusion reactions, culminating in the fusion of two helium-3 atoms into two protons and a helium-4 atom (4). This helium-3 fusion is the focus of this study due to its key implications for more efficient and sustainable fusion reactor design. Helium-3 fusion, unlike artificial fusion, does not produce any neutrons (4). These neutrons damage fusion reactors over time, making the reaction less sustainable in the long-term (5). Helium-3 fusion also allows us to directly convert the energy released by the fusion reactions directly into energy, bypassing the steam cycle (6). By understanding how the sun and other stars use this more efficient reaction, we can incorporate these principles to make our reactors more efficient.

Stellar and artificial fusion differ greatly in their required conditions. To achieve deuterium-tritium (D-T) fusion, fuel must reach approximately 150 million Kelvin (7). Powerful magnetic fields or similarly powerful lasers prevent this plasma from damaging or destroying the reactor, maintaining sufficient density for fusion (7, 8). For comparison, helium-3 fusion requires temperatures 175 times higher than D-T fusion to achieve similar reaction rates under laboratory conditions, yet the Sun's core is 10 times cooler (7, 9). This apparent contradiction raises the question: how can a star sustain fusion with a reaction that is seemingly more difficult at lower temperatures? The explanation lies in the immense fuel density of stellar cores (10).

In fusion, density describes the number of fuel atoms within a given volume. In stellar cores, extremely high gravitational forces compress matter to high densities around 150 g/cm^3 (11). Fusion arises from quantum interactions between atoms and thus is inherently complex (12). For fusion to occur, atoms must overcome the repulsive force that pushes protons apart (13). This force, known as the Coulomb force, is counteracted at very close distances by the strong nuclear force, which binds all atomic nuclei (14). The key challenge of fusion is bringing two nuclei close enough (about two proton's widths) for the strong force to dominate and merge the two nuclei (15, 16).

In fusion, an atom must hit a target atom. The Coulomb barrier—the force that repels two like-charged particles—would normally prevent the two atoms from combining. To overcome this barrier, the incoming atom must have enough energy, around 450 keV (12). Alternatively, the atoms can burrow straight through the barrier in a process known as quantum tunneling (17). The chances of successful tunneling increase as the atom's energy increases (10).

After getting past the barrier, the incoming atom must still hit the target atom. This is complicated by the fact that the energy of the target influences the available area that the incoming atom can hit. This target area is called the nuclear cross-section. Fusion reactions do not always become more efficient as temperatures increase; instead, different reactions have different optimum temperatures at which their fusion rate peaks (9). For artificial fusion, specifically the deuterium-tritium reaction, that temperature is approximately 835 million Kelvin (9, **Figure 1**). In contrast, for stellar fusion, where two

https://doi.org/10.59720/25-147

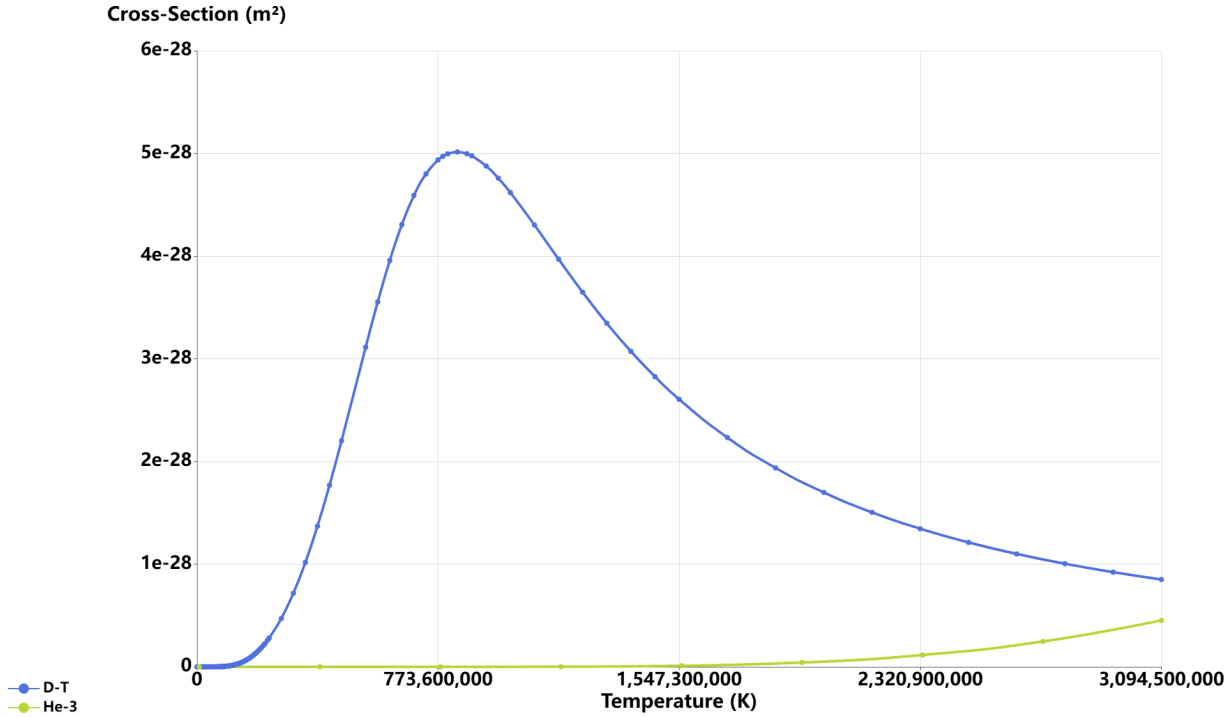

Figure 1. Fusion cross-sections of deuterium-tritium (D-T) and helium-3 (He-3) fusion reaction vs. fuel temperature. Fusion cross-sections in m^2 for D-T (blue) and He-3 (green) fusion reactions as a function of temperature in Kelvin. Graphed by converting raw cross-section data in terms of barns (1 barn = 10^{-28} m^2) and electron volts (1 eV = 1.60218e-19 Joules). Temperature was calculated using the formula for average molecular kinetic energy of a gas, $T = 2/3 * E * k_B$, where E is in terms of Joules.

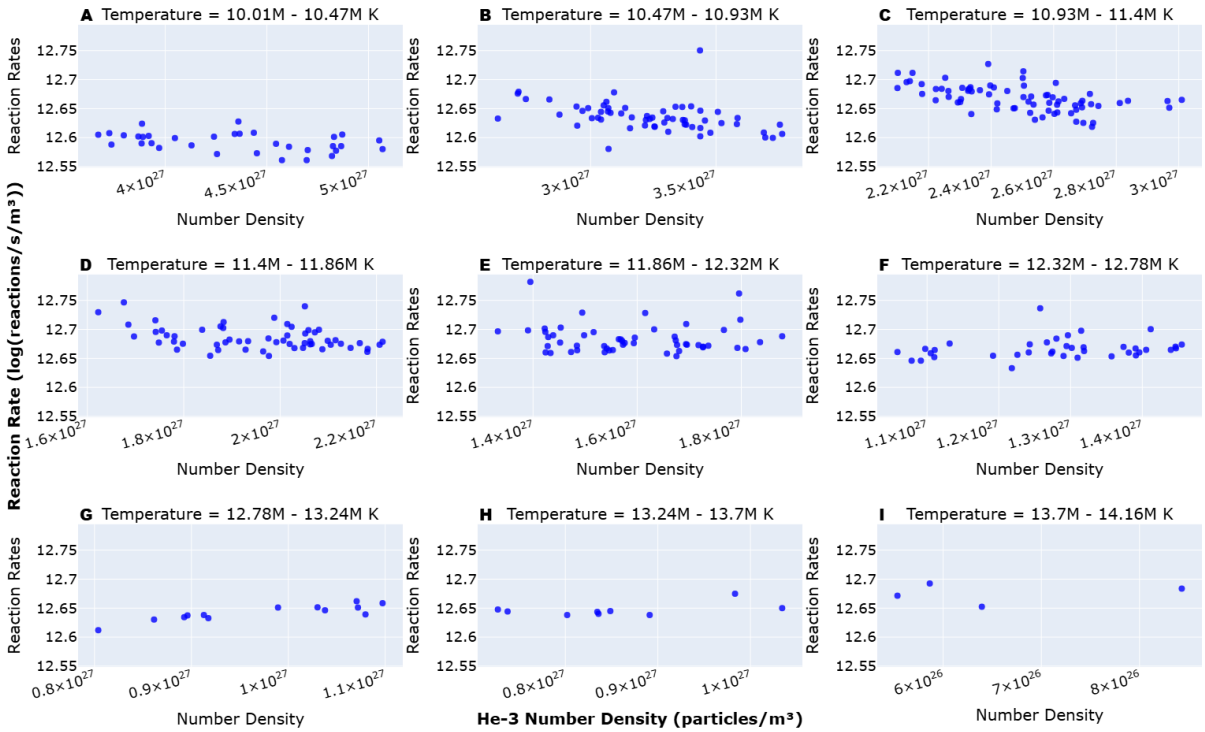

Figure 2. Reaction rates as a function of helium-3 (He-3) number density with varying temperatures. Graphs of reaction rates versus He-3 number density over (A) 10.01M–10.47M K, (B) 10.47M–10.93M K, (C) 10.93–11.4M K, (D) 11.4M–11.8M K, (E) 11.86M–12.32M K, (F) 12.32M–12.78M K, (G) 12.78M–13.24M K, (H) 13.24M–13.7M K, and (I) 13.7M–14.16M K temperature frames (n = 324). Equally sized slices were taken out of simulation results to aid in visualizing the 3-dimensional data analyzed in this project.

https://doi.org/10.59720/25-147

Term	Coefficient	t-statistic	p-value
Constant (reactions/s)	-4431.601421	0.397489	0.6912741
Number Density (m^{-3})	-1294.470482	-7.258733	3.034263×10^{-12}
Number Density Squared (m^{-6})	9.459420	7.220124	3.873692×10^{-12}
Core Temperature (K)	9236.588515	2.442044	0.01515053
Core Temperature Squared (K^2)	2031.078040	-4.124984	4.742070×10^{-5}
Core Temperature Cubed (K^3)	109.898367	4.865623	1.801230×10^{-6}
Interaction (m^{-3} K)	110.114593	7.275553	2.727231×10^{-12}

Table 1. Table of regression terms, their individual t-statistics, and their *p*-values. *P*-values are calculated with a two-tailed t-test with 317 degrees of freedom. The model F-test had an F statistic (6, 317) of 118.4 and an R^2 of 0.692.

helium-3 atoms fuse, the required temperature is so extreme that it has not yet been directly measured (9, **Figure 1**). In fusion, there is one more crucial factor: fuel density. The fuel density—the number of reacting particles per unit volume—dictates how many atoms are available as targets. More targets lead to higher fusion rates overall (10).

Given the complex interplay between temperature and density, no theoretical model currently exists for a direct relationship between temperature, density, and fusion reaction rates. Thus, an empirical model based on stellar data may provide new insights for fusion reactor design. This research aims to develop such a model by analyzing stellar core conditions through computational simulations. Stellar cores serve as an example of fusion as they exhibit both high temperatures and high densities, making them invaluable for studying how these parameters interact.

This study aims to investigate how density and temperature jointly affect fusion reaction rates by using stellar simulations to provide data on the star's fusion reactions and internal properties. We hypothesized that fusion reaction rates would increase with density, regardless of temperature. However, after nearly 1,892 simulations over the course of 36 hours, this prediction was found to be incorrect. While density exhibited a quadratic relationship with reaction rates, the effect was neither entirely positive nor independent of temperature. Instead, density and temperature interact to increase reaction rates to a greater degree than they would alone. These findings suggest that new reactor designs should focus on testing the validity of using high-density fuel in combination with a high-temperature reaction environment. If this principle holds true, humanity would be one major step closer to truly globalized green energy, which would help combat climate change.

RESULTS

To test how density and temperature affect reaction rates, we ran 1,892 simulations over the course of 36 hours using the simulation codes in the Modules for Experiments in Stellar Astrophysics (MESA) (18). MESA provided detailed information on internal stellar conditions, including fusion reactions, composition, temperature, and density (15). We collected the data for these simulations from the Gaia Collaboration's 3rd Data Release and the 17th Data Release of the APOGEE-2 dataset provided by the Sloan Digital Sky Survey (SDSS) (19, 20).

After filtering out data noise and outliers, we used the remaining 324 high-quality data points for modeling. Before constructing the model, we analyzed the data points visually to determine the best components for the model. We plotted the density versus reaction rate data over multiple temperature ranges. These plots revealed that temperature and density interact, meaning that temperature changes how density affects reaction rates and vice versa (**Figure 2**). To account for this, we added an interaction term (density times temperature) to the model. Running the regression using the statsmodels Python library produced the following model through an ordinary least squares regression (21):

$$\log(\hat{y}) = -1294.5\log(n) + 9.5\,(\log(n))^2 + 9236.6\,(\log(T)) - 2031.1\,(\log(T))^2 + 109.9\,(\log(T))^3 + 110.1(\log(n)\cdot\log(T)) - 4431.6 \quad (1)$$

In this equation, ŷ is the predicted reaction rate in reactions per second per cubic meter. *n* is the number density of helium-3 in particles per cubic meter. *T* is the temperature in Kelvin. The logarithm of the terms is taken for two reasons: to linearize data to make modeling easier, and to increase numerical stability, preventing the statsmodels library from returning negative R^2 values. Each term of the model was statistically significant at the $\alpha < 0.05$ level except for the constant (**Table 1**). This is acceptable since the constant has no true meaning in the model other than as an adjustment factor as fusion is not feasible without any fuel or a temperature of 0 Kelvin.

With an F statistic (6, 317) of 118.4, the model was statistically significant overall (p = 7.78 x 10-78) and moderately well-fitted to the data. With an R-squared of 0.692, the model accounts for approximately 69.2% of the variation in reaction rates due to changes in density, temperature, or their interaction. While the model generally matches the data, at high temperatures where data were sparse, the model over- or under-estimates the reaction rates (**Figure 3**). The model residual plots emphasize these errors (**Figure 4**). Further, in certain temperature ranges (*i.e.* panels **4G-H**), the model residuals showed a negative linear and a positive parabolic pattern, respectively, indicating that the model had data ranges where it did not fit the data well.

The interaction between temperature and density gave rise to several intriguing effects. Namely, density uniformly reduces reaction rates at low temperatures. As temperature increases, density exerts a smaller downward pressure on reaction rates. The relationship exhibits a pivot point around 3×10^{27} particles per cubic meter, beyond which density starts having a positive effect on reaction rates. With further temperature increases, this pivot becomes sharper and occurs at lower densities, until density ultimately acts to enhance reaction rates across all conditions (**Figure 5**).

DISCUSSION

In this study, we investigated stellar simulations to understand how temperature and density affect nuclear fusion in high-temperature, high-density environments. Data from 1,892 simulations showed an interdependent relationship

https://doi.org/10.59720/25-147

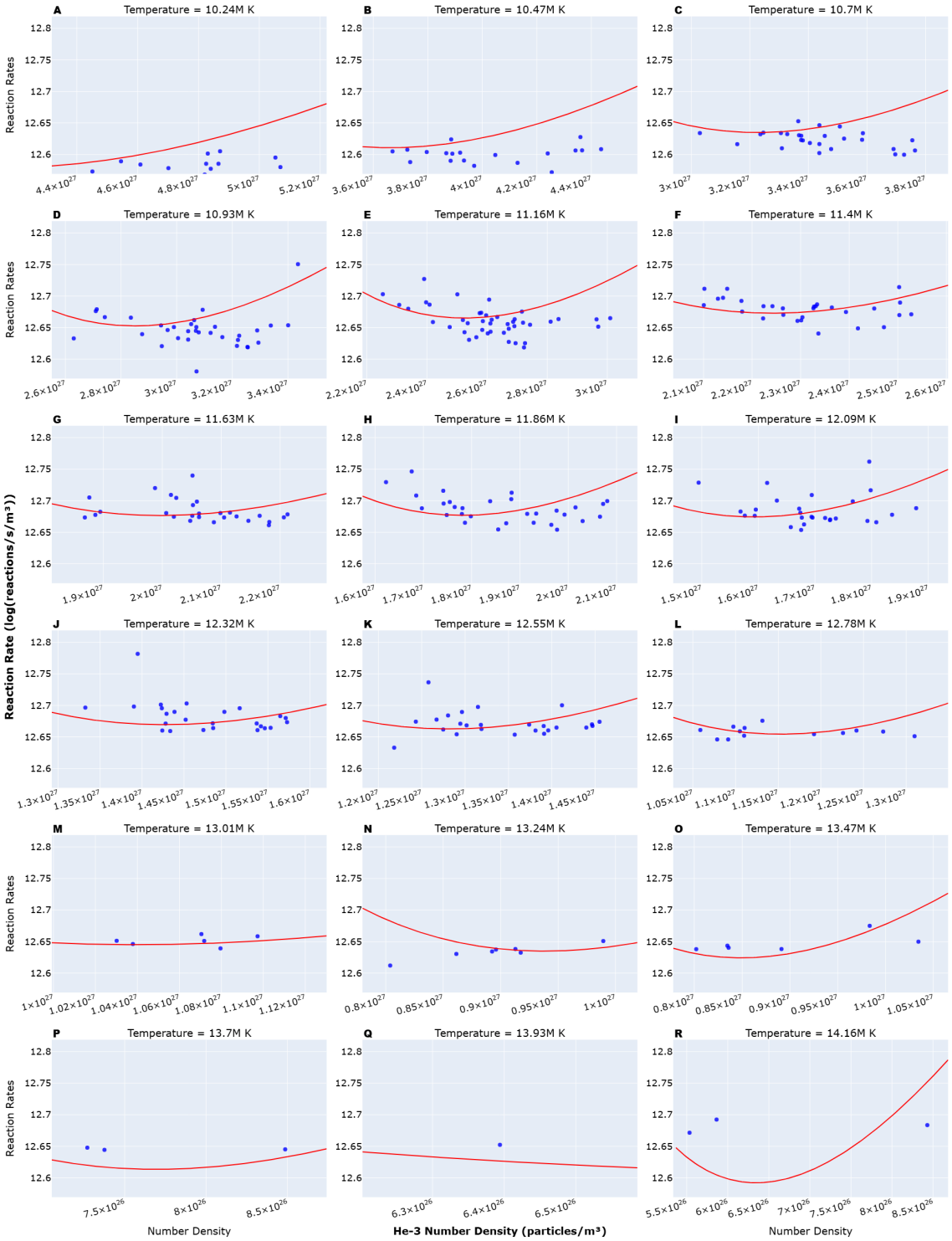

Figure 3. Model prediction for fusion reaction reactions as a function of density at different temperatures. Eighteen different graphs with the output of the regression model (red line) shown varying over density at a temperature of A) 10.24M K, B) 10.47M K, C) 10.7M K, D) 10.93M K, E) 11.16M K, F) 11.4M K, G) 11.63M K, H) 11.86M K, I) 12.09M K, J) 12.32M K, K) 12.55M K, L) 12.78M K, M) 13.01M K, N) 13.24M K, O) 13.47M K, P) 13.7M K, Q) 13.93M K, R) 14.16M K. Data points (blue dots) from stellar simulations encompassing the temperature range from A) 10.01M – 10.24M K, B) 10.24M – 10.47M K, C) 10.47M – 10.7M K, D) 10.7M – 10.93M K, E) 10.93M – 11.16M K, F) 11.16M – 11.4M K, G) 11.4M – 11.63M K, H) 11.63M – 11.86M K, I) 11.86M – 12.09M K, J) 12.09M – 12.32M K, K) 12.32M – 12.55M K, L) 12.55M – 12.78M K, M) 12.78M – 13.01M K, N) 13.01M – 13.24M K, O) 13.24M – 13.47M K, P) 13.47M – 13.7M K, Q) 13.7M – 13.93M K, R) 13.93M – 14.16M K are shown for comparison. The model F-test had an F statistic (6, 317) of 118.4 and a *p*-value of 7.76 x 10^{-78} which is far less than the 0.05 significance level.

https://doi.org/10.59720/25-147

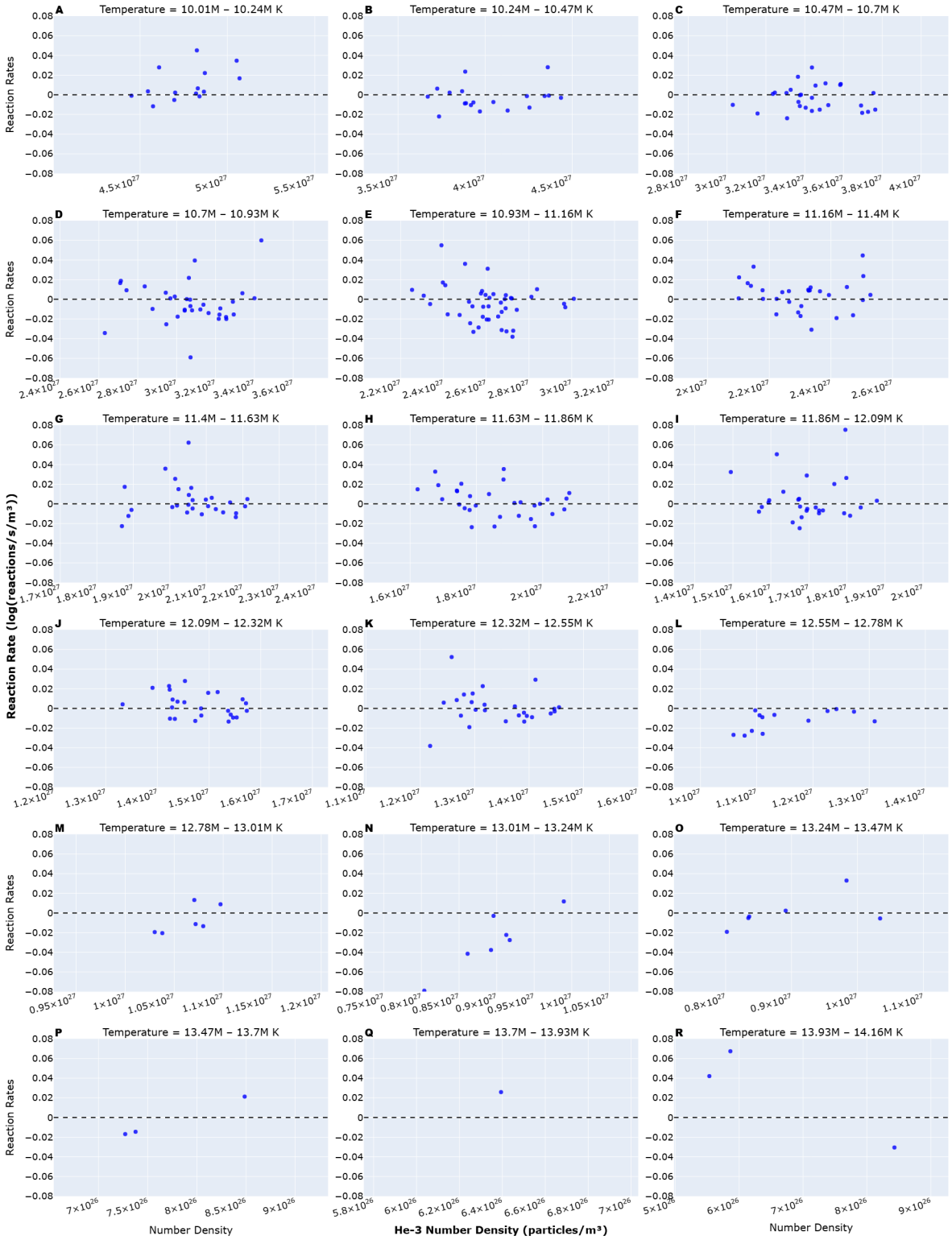

Figure 4. Regression residuals with density plotted against reaction rates with varying temperatures frames. Eighteen different graphs with the residuals (actual value minus regression model output) shown varying over density in temperature ranges A) 10.01M – 10.24M K, B) 10.24M – 10.47M K, C) 10.47M – 10.7M K, D) 10.7M – 10.93M K, E) 10.93M – 11.16M K, F) 11.16M – 11.4M K, G) 11.4M – 11.63M K, H) 11.63M – 11.86M K, I) 11.86M – 12.09M K, J) 12.09M – 12.32M K, K) 12.32M – 12.55M K, L) 12.55M – 12.78M K, M) 12.78M – 13.01M K, N) 13.01M – 13.24M K, O) 13.24M – 13.47M K, P) 13.47M – 13.7M K, Q) 13.7M – 13.93M K, R) 13.93M – 14.16M K. Data points (blue dots) represent an actual reaction rate minus a model prediction based on the temperature and helium-3 number density of that specific star.

https://doi.org/10.59720/25-147

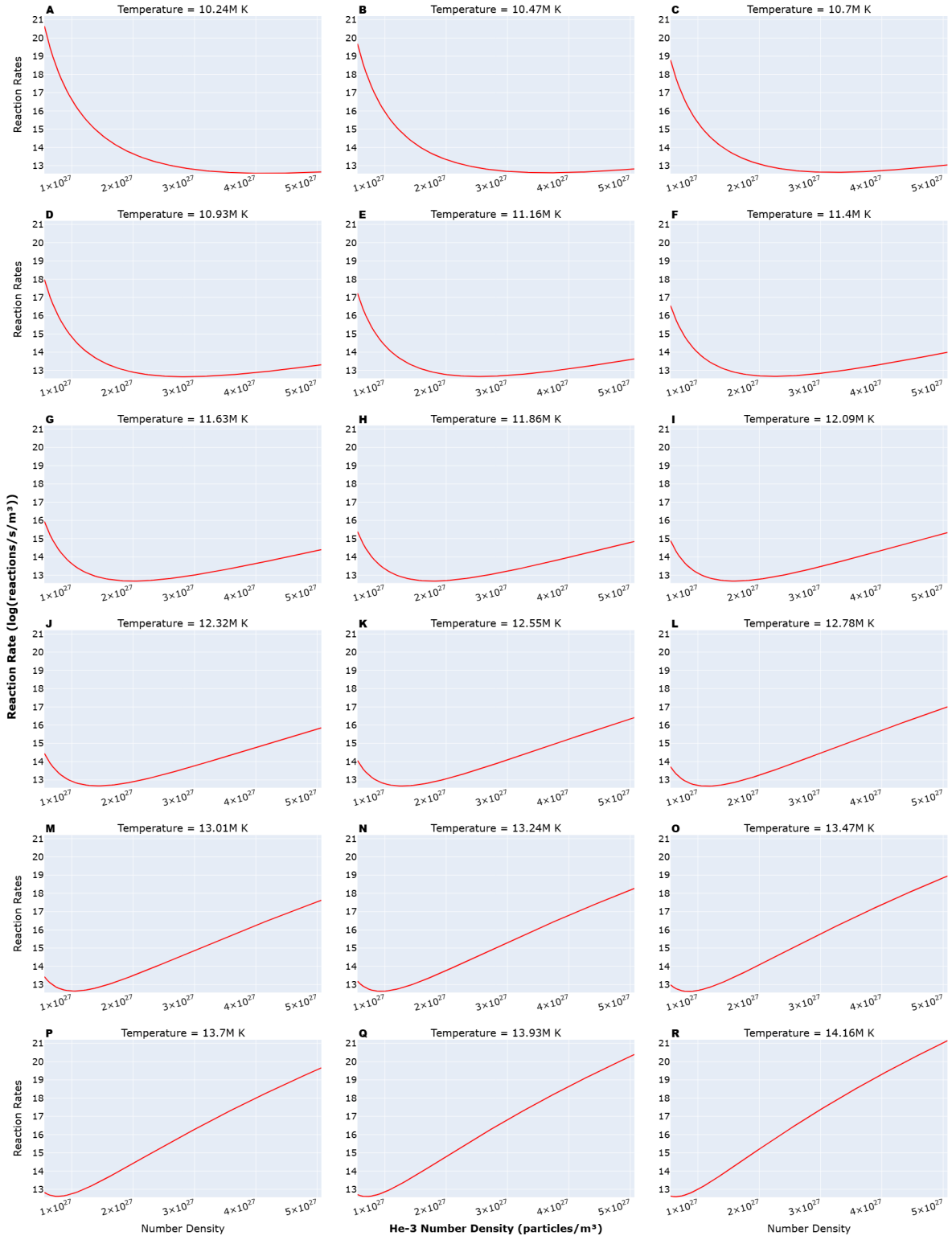

Figure 5. Extrapolated regression predictions with density plotted against reaction rates and varying temperature frames. Graphs of the regression model's predictions of reaction rates based on varied helium-3 number density. Eighteen graphs plotted on the same density interval from 5 x 10^{26} particles per cubic meter to 5 x 10^{27} particles per cubic meter. Each graph represents predictions made with the temperature listed above the graph as the basis for the temperature, temperature squared, and temperature cubed terms of the regression model. The temperatures are A) 10.24M K, B) 10.47M K, C) 10.7M K, D) 10.93M K, E) 11.16M K, F) 11.4M K, G) 11.63M K, H) 11.86M K, I) 12.09M K, J) 12.32M K, K) 12.55M K, L) 12.78M K, M) 13.01M K, N) 13.24M K, O) 13.47M K, P) 13.7M K, Q) 13.93M K, R) 14.16M K.

https://doi.org/10.59720/25-147

between the two parameters: increases in both temperature and density produced synergistic effects on fusion reaction rates that were greater than increases in either factor alone.

These findings partially support the initial hypothesis. As predicted, the relationship between density and reaction rates was quadratic; however, it was neither solely positive nor independent of temperature. The model predicted that increasing density at low temperatures leads to reduced reaction rates. This result may provide insight into cold fusion concepts (a controversial and unconfirmed method of achieving fusion at room temperature), which rely on novel confinement techniques to achieve extremely high densities (22, 23). This behavior aligns well with inertial confinement fusion (ICF), which uses powerful lasers to rapidly heat fuel to 100 million Kelvin for several nanoseconds while compressing it into densities over 1000 g/cm3 (24, 25). These temperatures and densities are an order of magnitude greater than stellar temperatures and densities; however, this peak temperature-density profile only exists for a few nanoseconds (24, 25). The nanosecond time frame limits the number of fusion reactions that can occur despite the extreme reaction rates, as reaction rates are measurements of reactions per second. Conversely, magnetically confined fusion (MCF) operates at temperatures in excess of 150 million Kelvin over the course of several seconds, but with fuel densities nearly a billion times lower than those achieved in ICF (26).

While ICF exhibits ideal temperature-density profiles, it cannot maintain these conditions long enough for net energy production. Other methods utilize high densities like cold fusion or high temperatures like MCF. Cold fusion does not work because the temperatures are too low for any measurable fusion events to occur, while MCF plasmas, despite running for several seconds, are so diffuse that they likewise still struggle to produce more energy than they consume.

However, considering that temperature and density did not account for 29.8% of the changes in reaction rates, it is more likely that the disparity between the model's predictions and the physics comes from confounding stellar mechanics. Stellar cores are dynamic objects that constantly mix with outer layers while undergoing a series of fusion reactions that ultimately create helium-4 (18). Additionally, stellar mass plays a major role in determining fusion reaction rates because higher masses lead to greater gravitational force, which in turn requires more fusion reactions to maintain equilibrium (27). Further research is necessary to control for these confounding factors.

We can control for the impact of core mixing and mass effects by changing how we create and analyze density-temperature profiles. Rather than comparing multiple stars at their current ages with varying stages of evolution, we would compare the same star to its past self. This new method would require re-running simulations with different data-tracking parameters but would yield data where mass is less of a confounding factor. Core mixing is another possible confounding factor, but this is only significant in stars greater than 1.1 times the mass of the Sun (28). By excluding such stars, core mixing's confounding effects would be mostly mitigated.

Another methodological improvement shifts from analyzing the absolute temperature, density, and reaction rates to analyzing changes in their quantities over time. If we used this approach, it remains unclear whether checking for divergence between the actual and simulated star would be necessary. In this study, such checks were performed because APOGEE-2 did not provide helium measurements, despite helium composing 20-30% of a typical star's mass (20, 29). Due to the input-sensitivity of stellar simulations, inaccurate helium predictions led many stars to diverge from their actual sizes. To illustrate this, we ran a pair of simulations based on solar compositions. The only difference is that one simulation would use helium and metallicity content based on our algorithm for predicting helium and the other would use compositions known to be present in the sun (29). The metallicities for both simulations differed by 4.4% and helium content differed by 0.41%. Both stars diverged in radius from the sun; however, the star with algorithmically determined helium and metallicity had a greater divergence—about 4.1% greater final reaction rate error relative to the star with more accurate composition. Divergence from stellar radius indicates inaccurate estimations of helium and metallicity. Thus, we excluded these divergent stars from the analysis. If self-comparison approaches still yield excessively noisy data, this issue could be mitigated by specifically targeting stars with known helium compositions.

The model also lacked many datapoints at high temperature, primarily due to the rarity of stars that primarily fuse hydrogen with correspondingly high temperatures. Remedying this problem is more complex: one could target high-temperature stars, but those stars tend to be more massive and, consequently, do not primarily fuse helium-3. Alternatively, more simulations could be run to expand the high-temperature dataset. Despite these limitations, the model is still a useful conceptual tool in reactor design as it shows how, in stars, fusion is an optimization problem of temperature and density. We need to solve this same optimization problem in our own reactors to make them more effective.

As stated previously, stars indicate that density decreases fusion reaction rates at low temperatures. However, at high temperatures, density is a strong positive factor in promoting higher reaction rates. This has two major implications for fusion reactor design. First, by utilizing higher densities and temperatures together, reactors can achieve greater efficiency beyond what temperature or density alone can provide. However, these efficiency gains would have limited value if reactors degrade rapidly during operation.

Second, density extends reactor lifetimes by enabling alternative fusion reactions such as stellar helium-3 fusion. As discussed earlier, the main reason that reactors degrade so quickly is that D-T fusion releases neutrons which strike reactor casings, damaging them over time (5). After only 5-10 years of full operation, these reactors must be decommissioned (30). In contrast, helium-3 fusion only releases protons that magnets can contain, preventing them from impacting and damaging reactor casing (4, 6). Instead of converting neutron energy into heat, into steam, and finally into electricity through a turbine, the moving protons create magnetic fluctuations which can be directly converted into electricity (6).

https://doi.org/10.59720/25-147

Helium-3 is a potentially better fusion reaction but requires much higher temperatures. However, as this model and stars themselves show, these energy requirements can be offset by using higher density fuel. Density facilitates more difficult reactions that are overall better for energy generation and long-term sustainable fusion pathways.

While these conclusions are based on stellar data, further validation is needed in the context of engineered fusion systems. To do this validation, we would need to simulate how different initial density and temperature profiles affected reaction rates inside of a fusion reactor. We can utilize these simulations to solve this fusion optimization problem.

Overall, this study demonstrates that density and temperature interact to increase reaction rates in stars. Changes in one variable change how the other variable influences reaction rates. This differs from the physics, in that density and temperature are treated as independent variables in the reaction rate equation. Together, increasing both density and temperature has a greater effect on reaction rates inside stars rather than optimizing them in isolation. Further research should focus on whether this trend similarly applies to the more controlled environment of fusion reactors. If it does, we have a new avenue to push fusion research forward, getting us one step closer to a green future.

MATERIALS AND METHODS

System and Software Requirements

This research used the Modules for Experiments in Stellar Astrophysics MESA (version r24.08.1) and the Python (version 3.11) programming language. The astropy (version 7), matplotlib (version 3.7.2), numpy (version 1.24.4), pandas (version 1.5.3), plotly (version 5.24.1), and statsmodels (version 0.14.4) packages were used extensively in this project (31, 32, 33, 34, 21). MESA is an industry-standard collection of tools for simulating stellar phenomena, ranging from atmospherics to stellar evolution. MESA was used to run stellar evolution to determine the internal profile of stars. Simulations modeled the life of the star from birth until a stopping condition, and required mass, initial composition, and that stopping condition. The stopping condition used in this research was based on the age of the star, though a fallback was chosen for if the star progressed into fusing helium rather than hydrogen. These helium-fusing stars were excluded before analysis. MESA models stellar fusion, its interactions with gravity, core mixing through convection, atmospherics, rotation, using an equation of state based on temperature and pressure (18). MESA outputs detailed profiles of the stellar interior, including detailed breakdowns of the temperatures, pressures, densities, reaction rates, and compositions of different radial regions within the simulated star. Stellar evolution codes are a robust method to get detailed fusion reaction information for an arbitrary mass and composition input.

MESA requires a Unix operating system to run properly, so the Linux operating system was used (18). The utility GNU Parallel was used to run multiple MESA simulations simultaneously (36). The system used for simulation had 8 CPU cores and 16 threads, so 4 simulations jobs were run simultaneously with each job allocated 4 threads.

Data Preparation

Gaia DR3 data was gathered directly from their query portal through the online Advanced Data Query Language (ADQL) interface. The query was used to gather all Gaia stars with a known mass, radius, and metallicity. The stars were further filtered to ensure they were in a hydrogen fusion stage by taking stars with an "evol_stage" parameter between 100–360. Since they fuse hydrogen, these stars also fuse helium-3 into helium-4, the reaction of focus for this study. The resulting query data—205,589 rows—was placed in the data folder. This data was stored in the repository so that it was not necessary to re-download this Gaia data.

Next, data was retrieved from SDSS; however, this is handled by the data preparation Jupyter notebook (mesa_data_prep.ipynb). Data were cleanly combined based on the Gaia star identifiers present in both the Gaia data and the APOGEE-2 data, giving 17,082 rows. Next, in accordance with SDSS recommendations and the literature, stars with possible error sources in measurements for iron, nitrogen, oxygen, carbon, magnesium, silicon, and sulfur were excluded, leaving 1,892 rows, after removing stars with duplicate identifiers (20, 37). Measurements of sodium, aluminum, potassium, calcium, chromium, manganese, and nickel were included if present and error-free. Including all these elements would lead to an estimate for metallicity (the fraction of mass of a star composed of elements heavier than helium) with an error of only 0.01% (37). These metallicity measurements were then used to estimate helium content based on formulations presented in the literature (37). The result of executing the data preparation notebook is a set of simulation inputs in the data.csv file in the simulation directory.

Simulations

To set up simulations, the template simulation was first built by running the "mk" file in the simulate/template directory (assuming MESA is properly installed). After running data preparation and customizing the number of threads and simulation jobs to match the system requirements, the "rn" file located in the simulate directory was run. This executed a series of Python and terminal scripts that orchestrate the simulations based on the template file provided in the **Appendix**. This template is not coded into MESA but was instead a custom-coded format where template arguments are replaced with appropriate values before the simulation is run. This is already part of the scripts that orchestrate the simulations. This template specifies that the simulation will use the specified mass and composition of that star. Further, the simulations will stop either when the age of the star matches the age provided by Gaia in the "age_flame" column or when the star runs out of hydrogen to fuse. Simulation results were outputted to the simulate/LOGS directory. The code repository already contains all raw data outputs used for the following analysis in this directory.

Analysis

After simulations were completed, analysis was performed in another Jupyter notebook (simulation_collation.ipynb). Raw simulation data were first pre-processed to extract data of interest, namely, identifier, mass, radius, age, core

https://doi.org/10.59720/25-147

radius, core mass, core volume, core temperature, core density, reaction rates per unit volume, core composition, and core helium-3 number density. This was accomplished by analyzing every simulated region of the star and taking mass-weighted averages of those zones' temperature, density, and composition, as well as the sum of the zones' fusion reaction rates divided by the core volume. This resulted in 1,892 datapoints, which were stored in the "stellar_profiles.json" so that they can easily be loaded again in the future.

The resulting simulation data were noisy, with only a faint trend present. This noise was most likely due to imprecise helium composition measurements. Since surveys like Gaia and APOGEE-2 do not measure helium content, an estimation was made based on mathematical methods (37). Errors in these estimations led to simulated stars that diverged in radius from the real star's radius, leading to high error levels in reaction rates per unit core volume. First, if the simulated star's age did not match the original star's age, it was excluded because this indicates that the star stopped fusing helium-3. This excluded 57 stars. Next, stars with high reaction rate error (> 5%) were excluded. We determined this 5% threshold based on testing different models; 5% yielded the most data points with clear trends while producing a very significant model. Lower thresholds had far less data and were not meaningfully more statistically significant. We calculated this error as such:

$$\text{error}=\left|\frac{r^3-\hat{r}^3}{r^3}\right|<5\% \qquad (2)$$

Where r is the actual radius, and $\hat{r}$ is the simulated radius. This equation is derived from how reaction rates depend directly on the core volume (cores are assumed to be perfect spheres), which is not calculated as an absolute value but as a proportion of the stellar radius. Errors in radius thus propagate to errors in reaction rates. This left 378 datapoints. Finally, to prevent outliers from skewing the results, outliers on reaction rates, temperature, and density were removed if they were greater than the 3rd quartile plus 1.5 times the interquartile range (IQR) or less than the 1st quartile minus 1.5 times the IQR of each respective quantity, leaving a total of 324 stars for analysis.

After filtering was complete, the model was constructed using the statmodels Python library with parameters for density, density squared, temperature, temperature squared, temperature cubed, their interaction, and the constant. The statsmodels Python library automatically performed an F-test and *t*-tests for each component and provided the appropriate statistic and *p*-value. All *p*-values were tested at the $\alpha = 0.05$ level. This model was then analyzed using a series of graphs produced with the plotly library.

The specific model was chosen based on a combination of the reaction rate equation, which relies on a quadratic density (which results in the quadratic density terms), and a visual analysis of the temperatures, which followed the shape of a cubic function. Additionally, it was found that using different variables, such as no interaction, quadratic/linear temperature, and additional interaction terms, led to statistically insignificant models.

The GitHub repository can be found here: https://github.com/max-widmaier/Stellar-Nuclear-Research

Received: April 29, 2025
Accepted: October 08, 2025
Published: June 19, 2026

REFERENCES

1. Miyamoto, Kenro. *Plasma Physics for Controlled Fusion*. Springer, 2016.
2. "Fission and Fusion: What Is the Difference?" *US Department of Energy*. Apr. 2021, https://www.energy.gov/ne/articles/fission-and-fusion-what-difference. Accessed 20 April 2025.
3. Lanctot, Mattheew. "DOE Explains... Fusion Reactions." https://www.energy.gov/science/doe-explainsfusion-reactions. Accessed 20 April 2025.
4. Clayton, Donald D. *Principles of Stellar Evolution and Nucleosynthesis*. University Press, 1983.
5. Knaster, J., et al. "Materials Research for Fusion." *Nature Physics*, vol. 12, no. 5, 2016, pp. 424–34, https://doi.org/10.1038/nphys3735.
6. Helion Energy. *Helion | FAQ*. 2024, https://www.helionenergy.com/faq/.
7. Breeze, Paul. *Nuclear Power*. Elsevier Science, 2017.
8. Lawrence Livermore National Laboratory. *How NIF Works*. https://lasers.llnl.gov/about/how-nif-works.
9. Brown, D. A., et al. "ENDF/B-VIII.0: The 8th Major Release of the Nuclear Reaction Data Library with CIELO-Project Cross Sections, New Standards and Thermal Scattering Data." *Nuclear Data Sheets*, vol. 148, 2018, pp. 1–142, https://doi.org/10.1016/j.nds.2018.02.001.
10. Hwang, Eunseok, et al. "Reinvestigating the Gamow Factor of Reactions on Light Nuclei." *The Astrophysical Journal*, vol. 955, no. 1, Sept. 2023, p. 79, https://doi.org/10.3847/1538-4357/acea80.
11. Hathway, David. *NASA/Marshall Solar Physics*. Sept. 2022, https://solarscience.msfc.nasa.gov/interior.shtml.
12. Nave, Carl R. *Coulomb Barrier for Nuclear Fusion*. 2017, https://hyperphysics.phy-astr.gsu.edu/hbase/NucEne/coubar.html.
13. Marion, Jerry B., and Mark A. Heald. *Classical Electromagnetic Radiation*. 2nd ed., Academic Press, 1980, pp. 1-33.
14. "DOE Explains...The Strong Force." *US Department of Energy*. https://www.energy.gov/science/doe-explainsthe-strong-force. Accessed 20 April 2025.
15. Pohl, Randolf, et al. "The Size of the Proton." *Nature*, vol. 466, no. 7303, July 2010, pp. 213–216, https://doi.org/10.1038/nature09250.
16. Salpeter, E. E. "The Effective Range of Nuclear Forces. Effect of the Potential Shape." *Phys. Rev.*, vol. 82, American Physical Society, Apr. 1951, pp. 60–66, https://doi.org/10.1103/PhysRev.82.60.
17. Flowers, P., et al. "Tunneling". *Chemistry LibreTexts*. 2023. https://chem.libretexts.org/Bookshelves/Physical_and_Theoretical_Chemistry_Textbook_Maps/Supplemental_Modules_(Physical_and_Theoretical_Chemistry)/Quantum_Mechanics/02._Fundamental_Concepts_of_

https://doi.org/10.59720/25-147

Quantum_Mechanics/Tunneling.
18. Paxton, Bill, et al. "Modules for Experiments in Stellar Astrophysics (MESA)." *The Astrophysical Journal Supplement Series*, vol. 192, no. 1, Dec. 2010, p. 3, https://doi.org/10.1088/0067-0049/192/1/3.
19. Gaia Collaboration, et al. "Gaia Data Release 3 - Summary of the Content and Survey Properties." *A&A*, vol. 674, 2023, p. A1, https://doi.org/10.1051/0004-6361/202243940.
20. Majewski, Steven R., et al. "The Apache Point Observatory Galactic Evolution Experiment (APOGEE)." *The Astronomical Journal*, vol. 154, no. 3, Sept. 2017, p. e94, https://doi.org/10.3847/1538-3881/aa784d.
21. Seabold, Skipper, and Josef Perktold. "Statsmodels: Econometric and Statistical Modeling with Python." *9th Python in Science Conference*, 2010. https://doi.org/10.25080/Majora-92bf1922-011.
22. Gilet, Candace, and Anna Thanukos. "Cold fusion." *Understanding Science*, https://undsci.berkeley.edu/cold-fusion-a-case-study-for-scientific-behavior/. Accessed 20 April 2025.
23. Gilet, Candace, and Anna Thanukos. "Cold fusion." *Understanding Science*, https://undsci.berkeley.edu/cold-fusion-a-case-study-for-scientific-behavior/the-ingenious-idea/. Accessed 20 April 2025.
24. Lawrence Livermore National Laboratory. "What Is the National Ignition Facility?" *NIF & PS*, https://lasers.llnl.gov/about/what-is-nif. Accessed 20 April 2025.
25. Rosen, Mordecai D. "The Long Road to Ignition: An Eyewitness Account." *Physics of Plasmas*, vol. 31, no. 9, Sept. 2024, p. 090501, https://doi.org/10.1063/5.0221005.
26. Moses, E. *Advances in Inertial Confinement Fusion at the National Ignition Facility (NIF)*. Vol. 85, Lawrence Livermore National Laboratory (LLNL), Livermore, CA, 10 2009, https://doi.org/10.1016/j.fusengdes.2009.11.006.
27. Jackiewicz, Jason. "Unit 9: Hydrostatic Equalibrium." *Astronomy 565: Stellar Structure and Evolution*, 17 September 2019. *Astronomy 565*, https://astronomy.nmsu.edu/jasonj/565/docs/09_17.pdf.
28. Dhillon, Vik. "phy213 - the evolution of stars - the evolution of high-mass stars." 27 Nov. 2012, https://vikdhillon.staff.shef.ac.uk/teaching/phy213/phy213_highmass.html.
29. Grevesse, N., et al. "The Solar Chemical Composition." *Space Science Reviews*, vol. 130, no. 1, 2007–6, pp. 105–14, https://doi.org/10.1007/s11214-007-9173-7.
30. Dose, G. "The Lifetime of Components in a Fusion Reactor." *Europhysics News*, vol. 52, no. 5, 2021, pp. 24–27, https://doi.org/10.1051/epn/2021503.
31. The Astropy Collaboration, et al. "The Astropy Project: Sustaining and Growing a Community-Oriented Open-Source Project and the Latest Major Release (v5.0) of the Core Package*." *The Astrophysical Journal*, vol. 935, no. 2, Aug. 2022, p. 167, https://doi.org/10.3847/1538-4357/ac7c74.
32. Hunter, J. D. "Matplotlib: A 2D Graphics Environment." *Computing in Science & Engineering*, vol. 9, no. 3, 2007, pp. 90–95, https://doi.org/10.1109/MCSE.2007.55.
33. Harris, Charles R., et al. "Array Programming with NumPy." *Nature*, vol. 585, no. 7825, Sept. 2020, pp. 357–362, https://doi.org/10.1038/s41586-020-2649-2.
34. McKinney, Wes. "Data Structures for Statistical Computing in Python." *Proceedings of the 9th Python in Science Conference*, edited by Stéfan van der Walt and Jarrod Millman, 2010, pp. 56–61, https://doi.org/10.25080/Majora-92bf1922-00a.
35. Plotly Technologies Inc. *Collaborative Data Science*. Plotly Technologies Inc., 2015, plot.ly.
36. Tange, Ole. *Gnu Parallel 2018*. Zenodo, 2018, https://doi.org/10.5281/zenodo.1146014.
37. Hinkel, Natalie R., et al. "A Concise Treatise on Converting Stellar Mass Fractions to Abundances to Molar Ratios." *The Astronomical Journal*, vol. 164, no. 6, Nov. 2022, p. 256, https://doi.org/10.3847/1538-3881/ac9bfa.